

Supporting Information:

NMRlipids IV: Headgroup & glycerol backbone structures, and cation binding in bilayers with PS lipids

Pavel Buslaev,[†] Tiago M. Ferreira,[‡] Ivan Gushchin,[†] Matti Javanainen,[¶] Batuhan Kav,[§] Jesper J. Madsen,^{||} Markus Miettinen,[§] Josef Melcr,[¶] Ricky Nencini,[¶] O. H. Samuli Ollila,^{*,¶} and Thomas Piggot **Authorlist is not yet complete[#]**

[†]*Moscow Institute of Physics and Technology*

[‡]*Halle, Germany*

[¶]*Institute of Organic Chemistry and Biochemistry, Academy of Sciences of the Czech Republic, Prague 6, Czech Republic*

[§]*Potsdam, Germany*

^{||}*Department of Chemistry, The University of Chicago, Chicago, Illinois 60637, United States of America*

[⊥]*Institute of Biotechnology, University of Helsinki*

[#]*Southampton, United Kingdom*

E-mail: samuli.ollila@helsinki.fi

S1 Simulated systems

S1.1 CHARMM36

POPC bilayer By Fernando Favela at <http://dx.doi.org/10.5281/zenodo.16830>

DOPS and POPS bilayers.

The data in Table I and Refs 1–3 [T. Piggot, please write simulation details](#)

POPC:POPS mixtures without additional ions

Simulations of POPC:POPS (5:1) mixture containing total 132 (110:22) lipids with potassium and sodium countertions were ran using CHARMM36 force field. The data are available from Refs. 4 and 5, respectively[T. Piggot, please write simulation details](#).

Simulations of POPC:POPS (5:1) ans POPC:POPS (1:1) mixtures containing total 300 lipids with potassium countertions were ran using CHARMM36 force field. The data are available from Refs. ? [J. Madsen, please write simulation details](#).

POPC:POPS (5:1) mixtures with additional monovalent ions

POPC:POPS (5:1) mixtures containing total 132 (110:22) lipids were simulated with the additional potassium and sodium countertion concentrations of ~450 mM and 890 mM using CHARMM36 force field at 298 K. The data, force field and input files generated using parameters given by CHARMM-GUI^{6,7} are available from Refs. 8–11.

POPC:POPS (5:1) mixtures with additional calcium

POPC:POPS (5:1) mixtures containing total 300 (250:50) lipids were simulated with the additional calcium concentrations [J. Madsen, please write simulation details](#).

S1.2 CHARMM36ua

DOPS and POPS bilayers.

The data in Table I and Refs 12,13 T. Piggot, please write simulation details

S1.3 MacRog

POPS bilayers.

The data in Table I and Refs 14,15 T. Piggot and M. Javanainen, please write simulation details

POPC:POPS (5:1) mixtures with additional potassium ions

The data in Table II and Refs 16,17 M. Javanainen, please write simulation details

S1.4 Lipid17

DOPS and POPS bilayers.

The data in Table I and Refs 18–21 B. Kav and M. Miettinen, please write simulation details

POPC:POPS (5:1) mixtures with additional potassium and sodium ions

The data in Table II and Refs 22–25 B. Kav and M. Miettinen, please write simulation details

POPC:POPS (5:1) mixtures with additional calcium

The data in Table II and Refs 26 J. Melcr, please write simulation details

S1.5 Slipids

To be written by Piggot and Favela

S1.6 Berger

To be written by Piggot and Ollila Simulations with excess sodium were taken directly from Ref. 27 and simulations with calcium directly from 28. Simulation of POPC at 310 K was taken directly from Ref. 29.

S1.7 GROMOS-CKP

To be written by Piggot CKPM refers to the version with Berger/Chiu NH₃ charges compatible with Berger (i.e. the NH₃ group having the same charges as in the N(CH₃)₃ group of the PC lipids; 'M' stands for Mukhopadhyay after the first published Berger-based PS simulation that used these charges³⁰) and CKP refers to the version with more Gromos compatible version (i.e. the charges for the NH₃ group taken from the lysine side-chain).

S2 Electrometer concept in PC lipid bilayers mixed with negatively charged lipids

The electrometer concept is based on the empirical observations that the order parameters of α and β carbons in PC lipid headgroup decrease (increase) proportionally to the bound positive (negative) charge^{31–34} (Fig. S1). Therefore, the headgroup order parameters can be used to measure the ion binding affinity to lipid bilayers containing PC lipids.^{31–33,35–37} Changes of the headgroup order parameters of other lipids with bound charge, like negatively charged PS and PG lipids, are also systematic, but less well characterized.^{35–38} Therefore, the ion binding affinity to negatively charged bilayers can be better characterized measuring the PC headgroup order parameters from mixed bilayers.^{35–39}

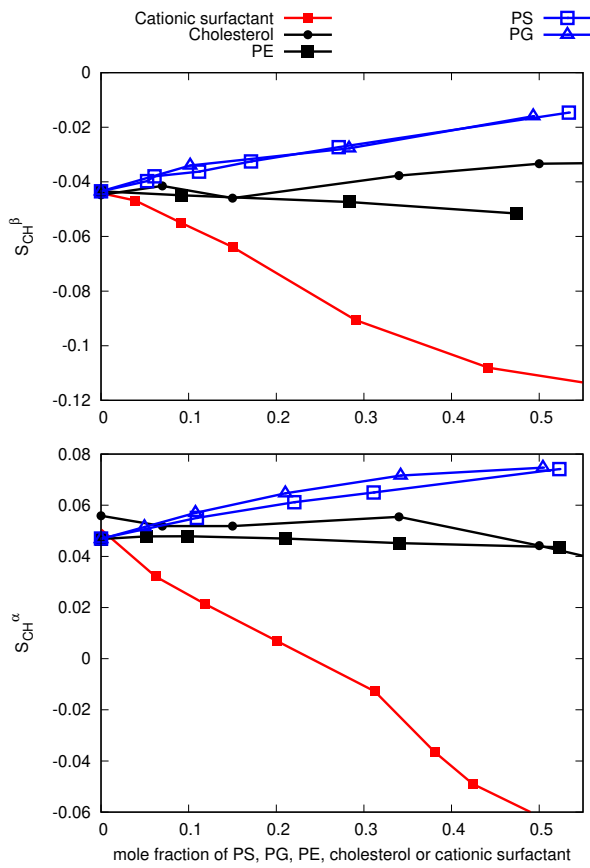


Figure S1: Headgroup order parameters of POPC measured from mixtures with PS (bovine brain), POPG, POPE, cholesterol and cationic dihexadecyldimethylammonium bromide (DHAB) surfactant.^{34,40,41} Signs are taken from separate experiments.^{42,43}

When comparing ion binding measured from the PC headgroup order parameters between neutral and anionic membranes, it is important to note that the order parameters increase due to the addition of negative charged lipids according to the electrometer concept^{33,40} (Fig. S1). Therefore, the headgroup order parameters of POPC in mixtures with anionic lipids are larger than in pure POPC lipid bilayer, which is also seen in the ion binding experiments from different mixtures in the absence of added calcium (Fig. S2). Upon addition of CaCl₂, the order parameters decrease and reach the values of pure PC bilayer close to the CaCl₂ concentrations of ~ 50-300mM, depending on the amount of negatively charged lipids in the mixture (Fig. S2). Around these concentrations the positive charge of bound Ca²⁺ cancels the negative charge lipids, resulting to a neutral membrane. Above such concentrations, the specific binding of calcium leads to the overcharging of the membrane.

Because the POPC headgroup order parameters in mixtures with different amounts of anionic lipids but without additional salt are not equal, the binding affinity of calcium can be better compared by plotting the changes of order parameters as a function of added calcium. As expected, such a plot reveals more pronounced order parameter decrease in systems with larger fractions of negatively charged lipids (Fig. S3), indicating an increase in the calcium binding affinity with the increasing amount of negatively charged lipids in membranes. In conclusion, the presented empirical comparison of headgroup order parameter changes from various mixtures of POPC and anionic lipids with added calcium gives physically consistent results, suggesting that the electrometer concept can be used to determine the cation binding affinity also to the lipid bilayers containing mixtures of PC and anionic lipids.

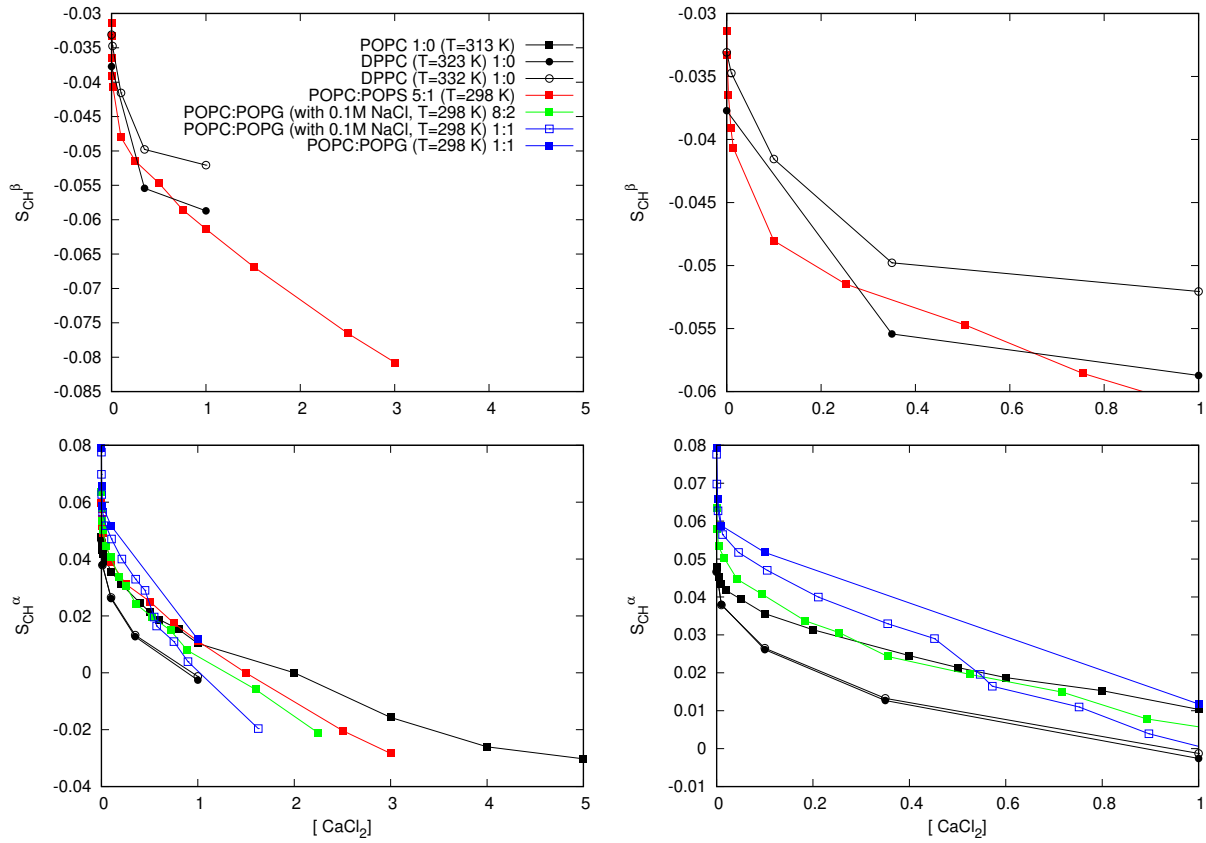


Figure S2: Headgroup order parameters of POPC as a function of CaCl concentration from experiments different mole fractions of negatively charged lipids (left column). Right column shows the same data zoomed to the concentrations below 1M. Data for Pure DPPC from,³¹ for pure POPC from,³² for POPC:POPS (5:1) mixture from,³⁷ for POPC:POPG (8:2,1:1) mixtures with 0.1M NaCl from³⁶ and for POPC:POPG (1:1) mixture data without NaCl from.³⁵

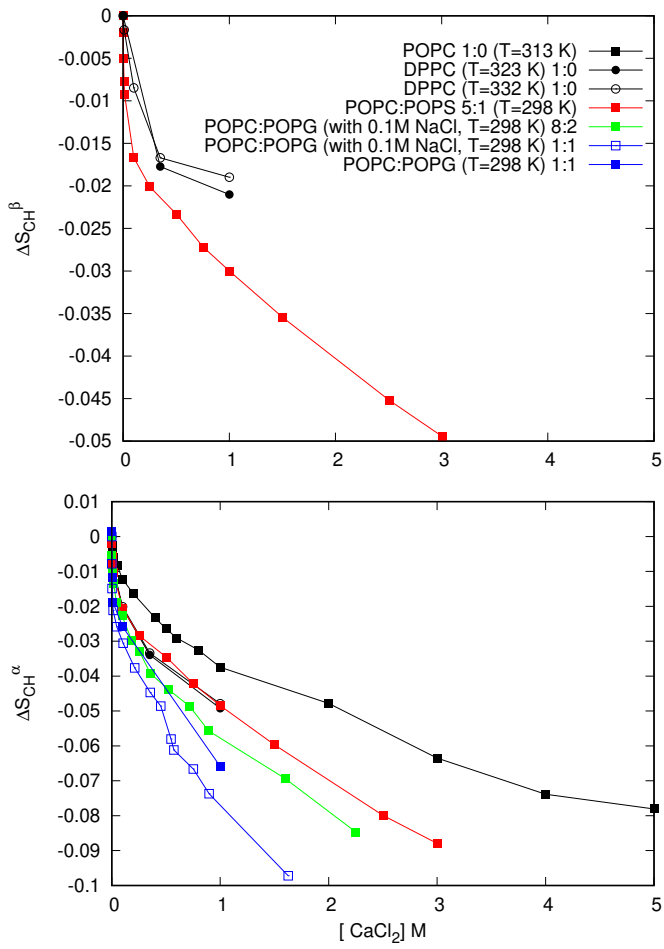


Figure S3: Changes of POPC headgroup order parameters as a function of CaCl_2 measured from mixed bilayers containing different amounts of anionic lipids. The original data is the same as in figure S2.

S3 Calibration of PC headgroup order parameter response to the bound cations

Before using the headgroup order parameters to compare ion binding affinity between simulations and experiments, the response of the order parameters to the bound charge in simulations should be quantified against experiments.^{44,45} In our previous work,⁴⁴ the ratio $\Delta S_{\text{CH}}^{\beta}/\Delta S_{\text{CH}}^{\alpha}$ was in good agreement with the experiments³¹ in the Lipid14 model, but was underestimated by other models. In the more recent study,⁴⁵ the headgroup order parameter responses were compared more carefully with the experiments of cationic dihexadecyldimethylammonium bromide (DHAB) surfactants in POPC bilayer.³⁴ The comparison reveals that the both headgroup order parameters in the Lipid14 model are too sensitive to the bound charge, while CHARMM36 gives better agreement for the α carbon (Fig. S4). Therefore, the headgroup order parameter response to the bound charge is actually more realistic in CHARMM36 model than in the Lipid14. In the latter, both order parameters are equally too sensitive to the bound cations giving a good result for the $\Delta S_{\text{CH}}^{\beta}/\Delta S_{\text{CH}}^{\alpha}$ ratio. The ratio was overestimated for the CHARMM36 model because the β -carbon order parameter is relatively more sensitive than the α -carbon order parameter. These results have to be taken into account when analysing the ion binding affinities using headgroup order parameters in simulations. However, we conclude that the discrepancies arising from the sensitivity of lipid headgroup to bound charge are typically smaller than the discrepancies arising from ion binding affinity.

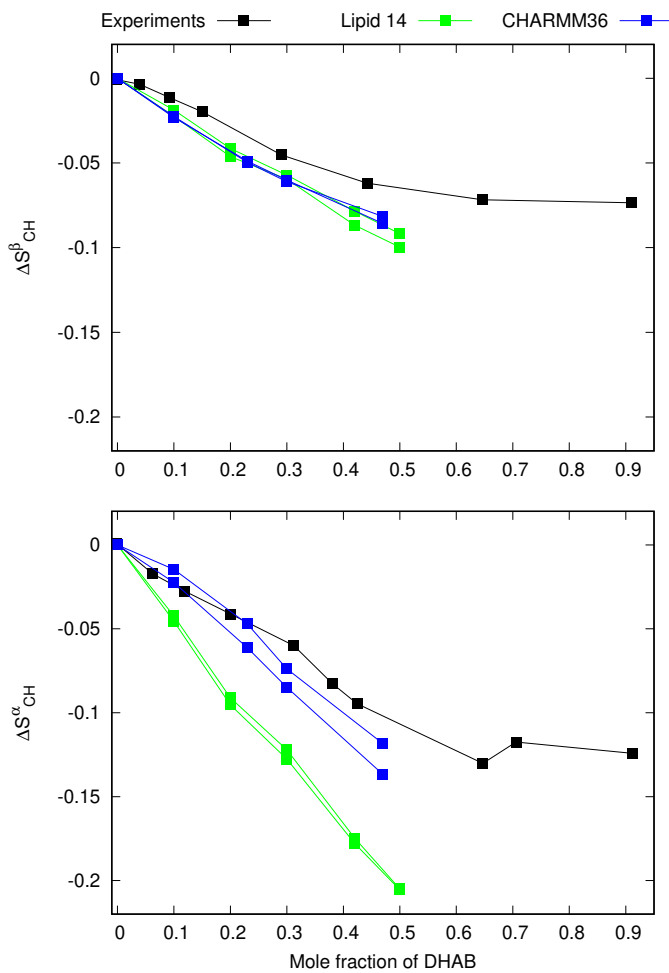


Figure S4: Responses of headgroup order parameters to the fixed amount of cationic surfactants in POPC bilayer from simulations and experiments.³⁴ The simulation results for Lipid14 are directly from Ref. 45. The CHARMM36 simulation data and details are available from Ref. 46.

S4 Effect of the definition of concentration on the headgroup order parameters as a function of ion concentration.

Previous studies using the electrometer concept to assess the ion binding affinity to lipid bilayers report ion concentrations either in water before solvating the lipids (buffer concentration)^{31,37,44} or in bulk water after solvating the lipids (bulk concentration).^{32,45} In this work, we use the former definition to be consistent with the reference experimental data.³⁷ The difference between these two concentrations increases with the increasing ion binding affinity. However, the difference is essentially negligible in the recent model⁴⁵ with realistic ion binding affinity (Fig. S5).

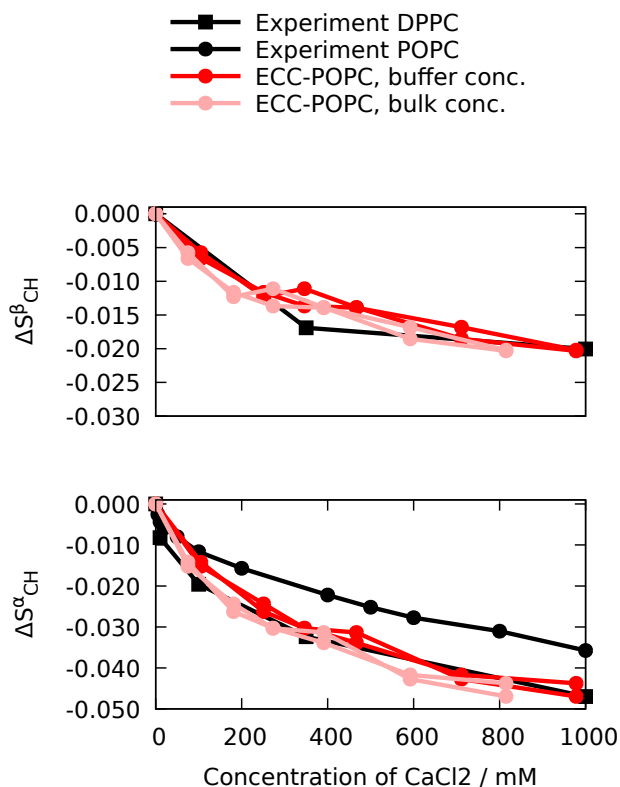


Figure S5: Changes of the headgroup order parameters as a function of CaCl_2 concentration using two possible definitions of ion concentration from the recent force field with realistic calcium binding affinity to a POPC bilayer⁴⁵ together with the experimental data.^{31,32}

S5 Dipolar slices of the R-PDFL experiment

Slices of the R-PDFL spectra (Fig. S6) show a single splitting for the β -carbon with the order parameter value of 0.11, and a superposition of a large and a very small splitting for the α -carbon. The larger splitting from the α -carbon gives a order parameter value of 0.09, while the numerical value from the small splitting cannot resolved with the available resolution.

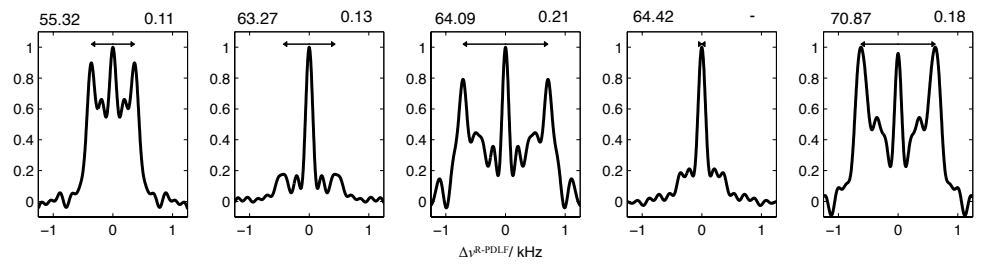


Figure S6: Dipolar coupling slices from the R-PDFL experiment.
Labeling of carbons and explanations of numbers (chemical shift and order parameter) would be good. The splitting corresponding the larger α -carbon order parameter should be also shown. Also, the size of the figure in the file may not be optimal.

S6 Dihedral angle distributions of the headgroup and glycerol backbone regions of PS lipids from different simulation models

The dihedral angles and structures of the glycerol backbone and headgroup regions of POPS lipids show wide variety between different simulation models (Figs. S7, S8 and S9). Detailed discussion of the structural differences is limited by the lack of realistic model that would correctly reproduce the headgroup and glycerol backbone order parameters. However, some structural characteristics of PS headgroup can be suggested based on the best available models (Figs. S10, S11 and S12), as discussed in the main text. The glycerol backbone structures are not discussed in this works because our focus is on PS headgroup. However, the data presented here can be useful for future investigations.

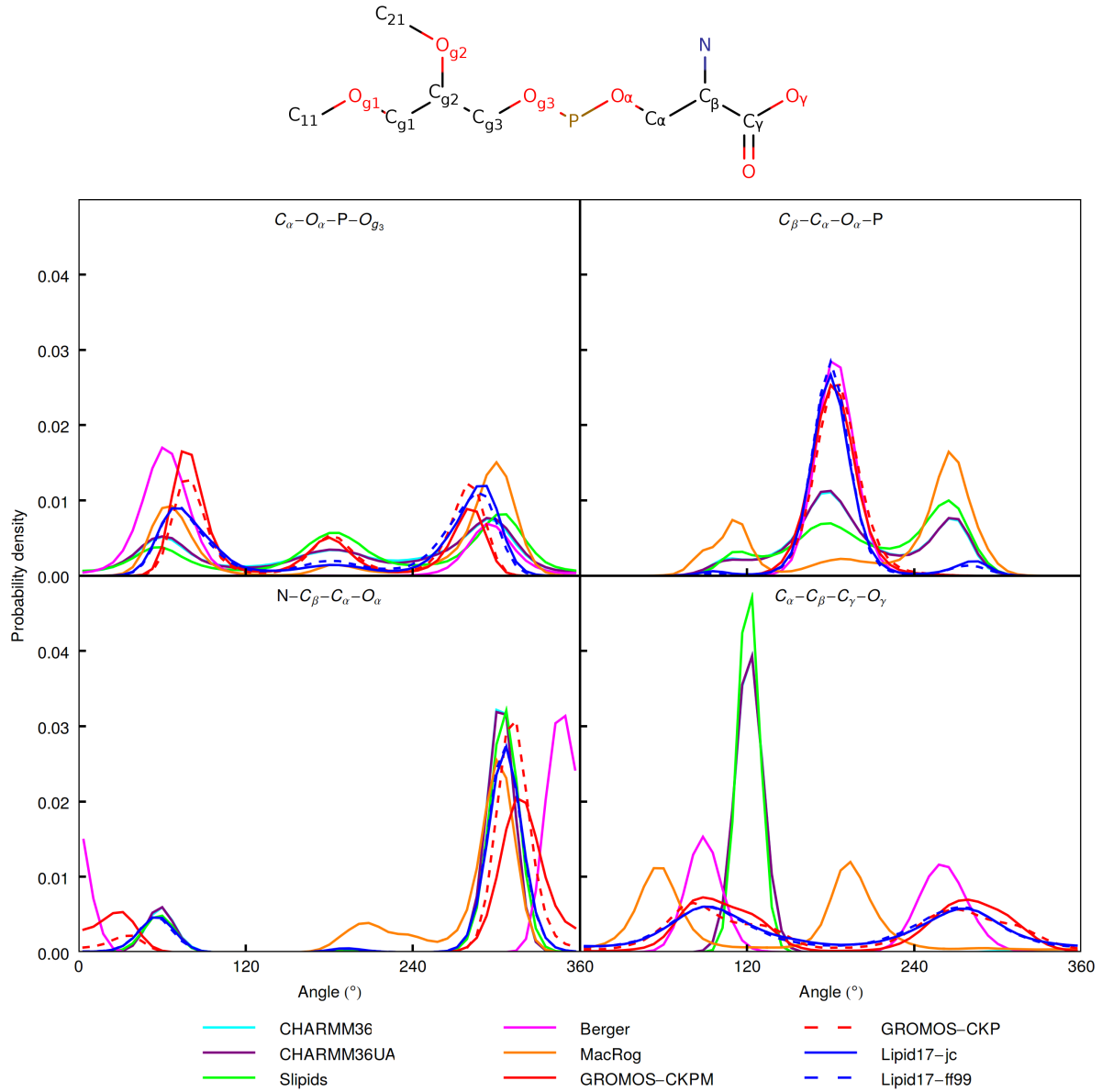


Figure S7: Dihedral angle distributions of the headgroup region of POPS from different simulation models.

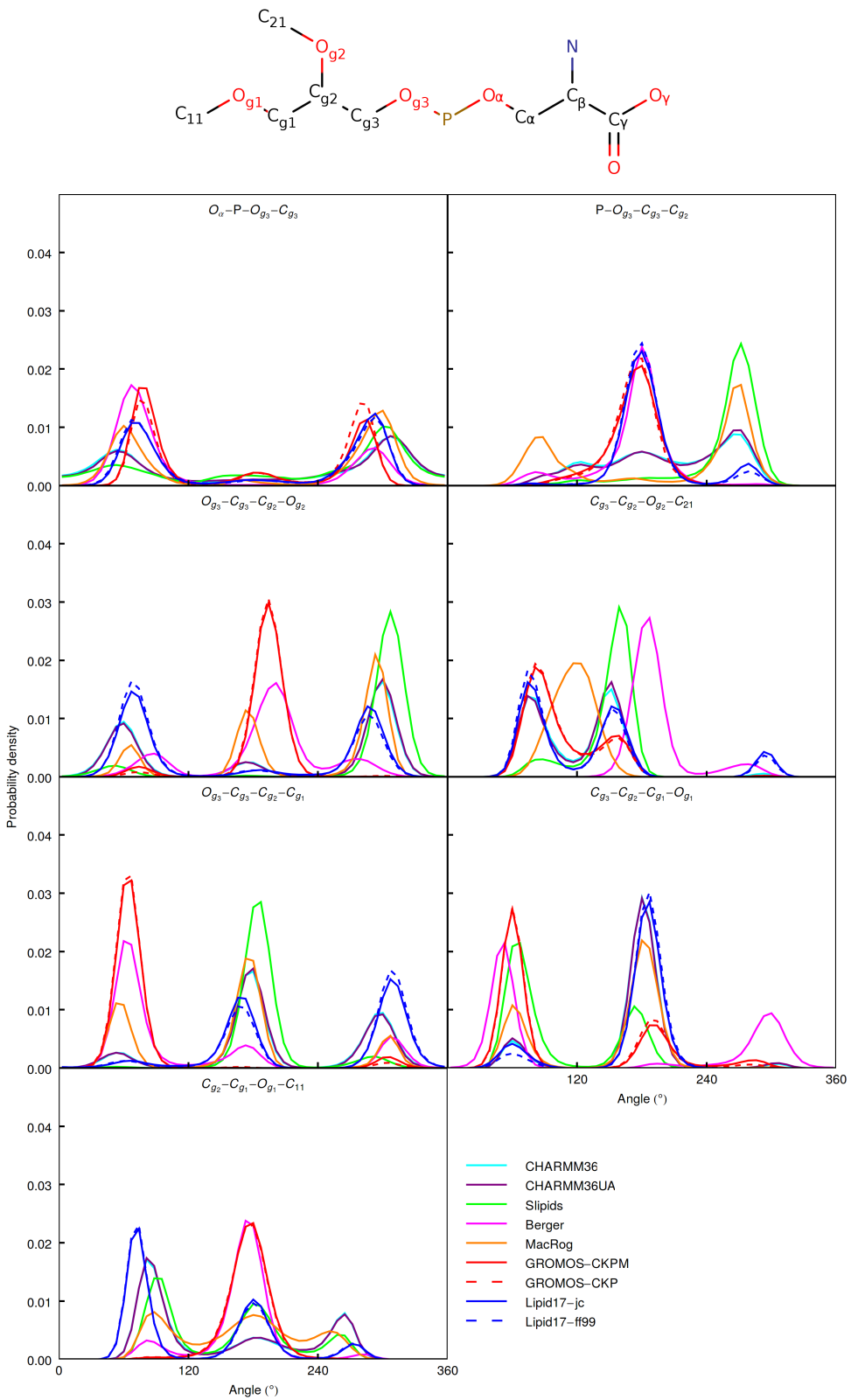


Figure S8: Dihedral angle distributions of the glycerol backbone region of POPS lipids from different simulation models.

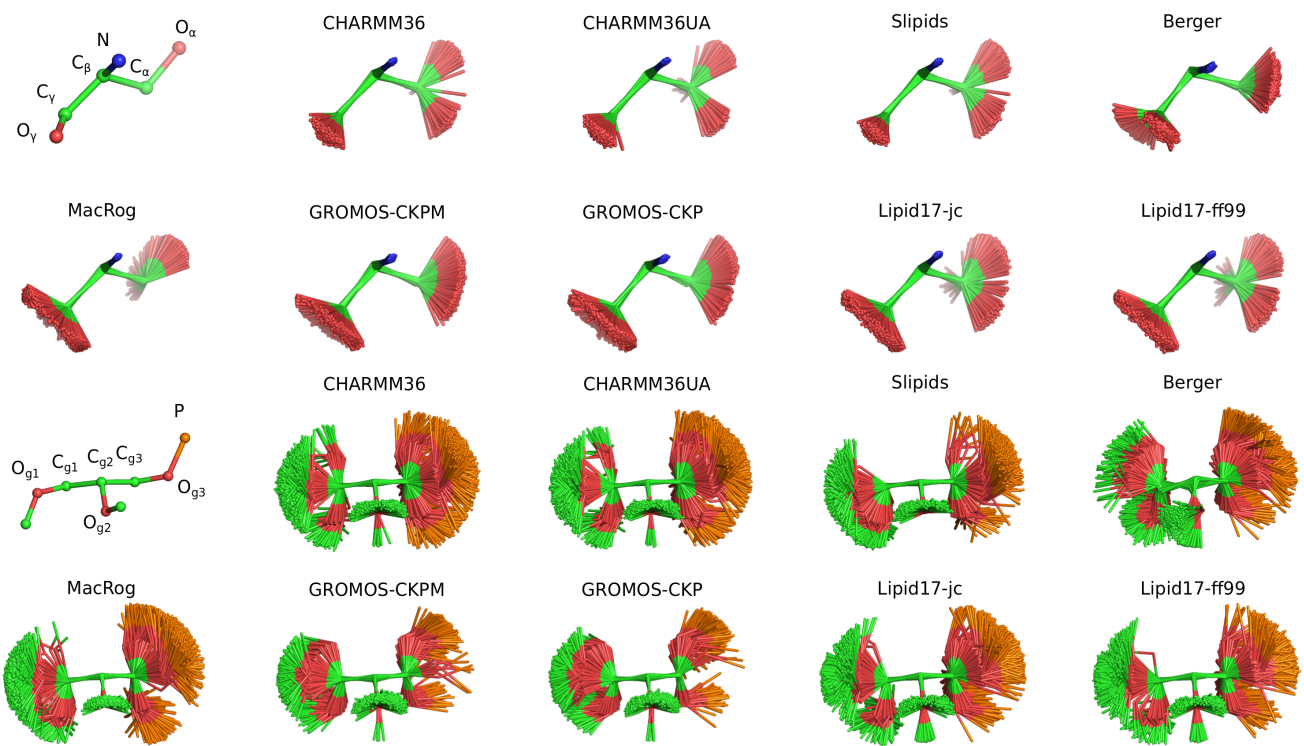


Figure S9: Overlayed snapshots of the glycerol backbone and headgroup regions from different POPS simulations.

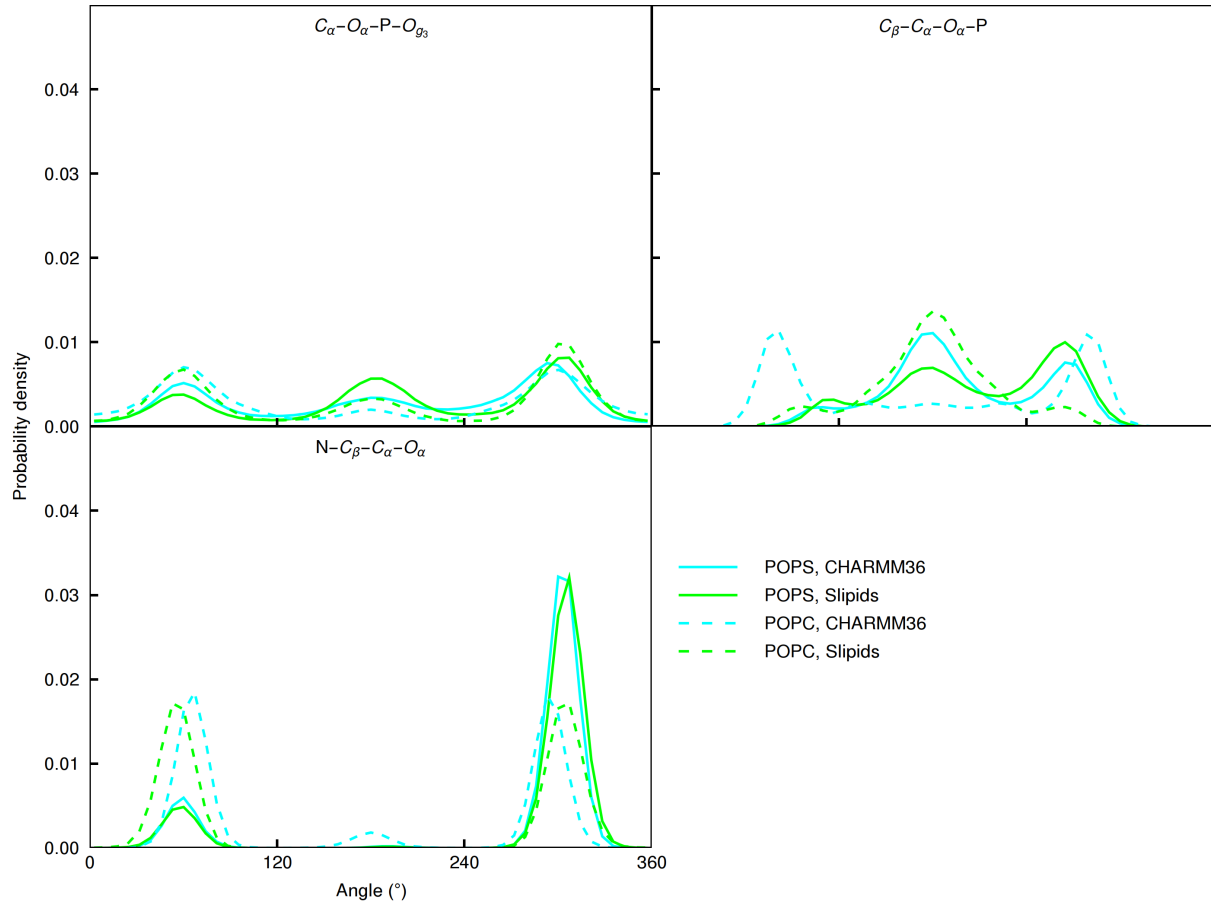


Figure S10: Dihedral angle distributions of the headgroup regions from CHARMM36 and Slipids simulations compared between the POPC and POPS lipids. The CHARMM36 POPC simulation is from Ref. 47 and Slipids POPC from Ref. 48.

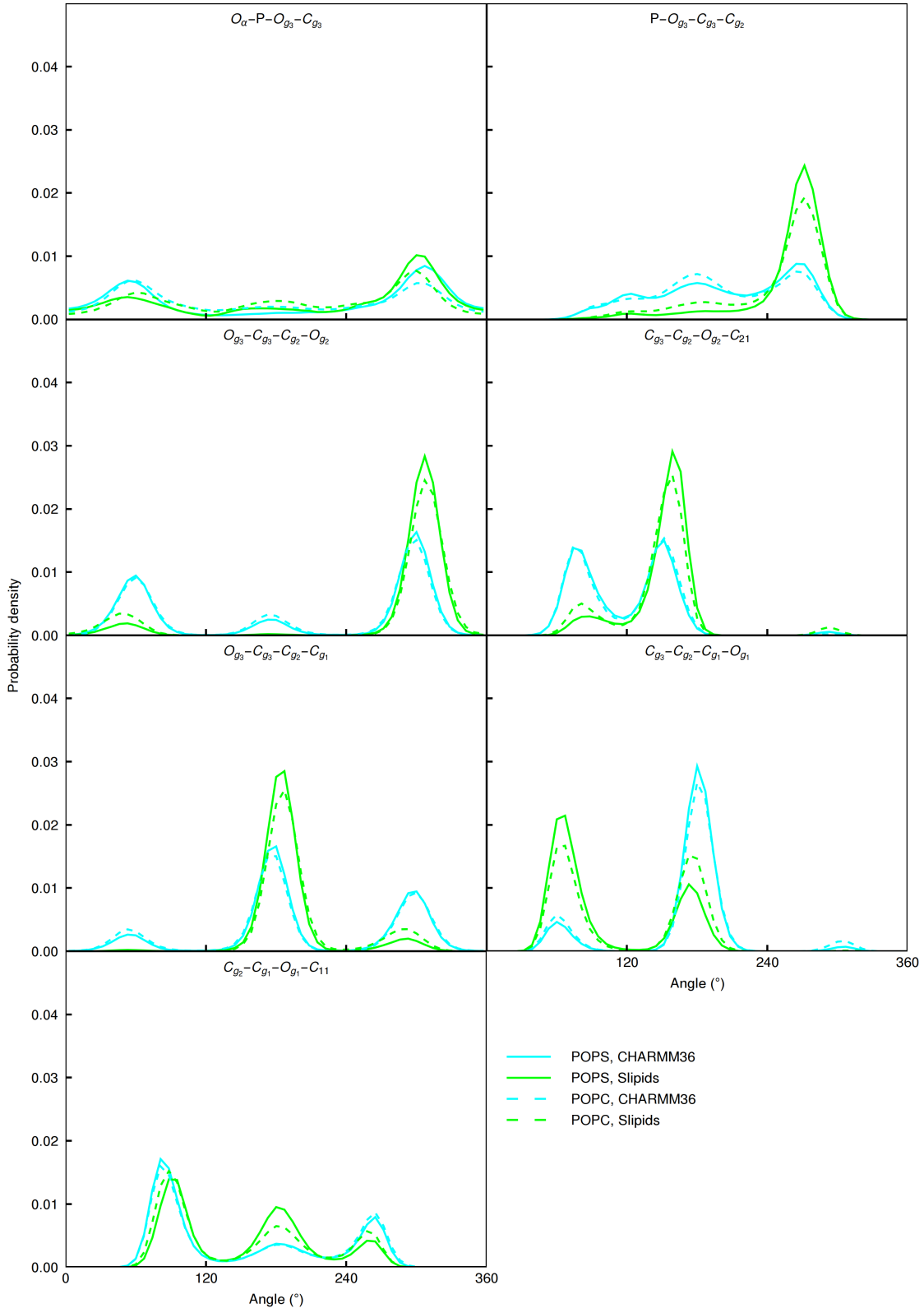


Figure S11: Dihedral angle distributions of the glycerol backbone regions from CHARMM36 and Slipids simulations compared between the POPC and POPS lipids. The CHARMM36 POPC simulation is from Ref. 47 and Slipids POPC from Ref. 48.

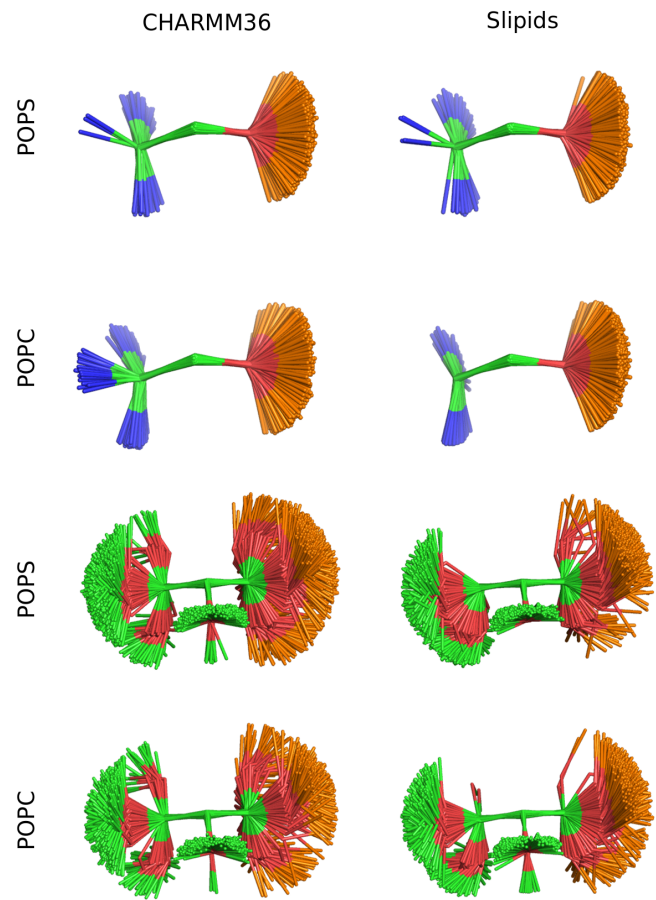


Figure S12: Overlayed snapshots of the headgroup and glycerol backbone regions from CHARMM36 and Slipids simulations compared between the POPC and POPS lipids. The CHARMM36 POPC simulation is from Ref. 47 and Slipids POPC from Ref. 48.

S7 Headgroup response to the additional counterions in POPC:POPS (5:1) mixtures

To evaluate counterion binding in different simulation models against experimental data,³⁷ we plot the headgroup order parameters measured from POPC:POPS 5:1 mixture as a function of different monovalent ions added to the buffer (Fig. S13). Experimental order parameters of POPC headgroup in the mixture are available as a function of LiCl and KCl concentrations, while POPS headgroup order parameters are measured also as a function of NaCl. Lithium interacts more strongly with PS headgroups than other monovalent ions,^{37,38,49–51} as also observed for PC headgroups.⁵² The different binding behaviour is evident also in the changes of PS headgroup order parameters, which decrease with the addition of lithium but increase with the addition of sodium or potassium (Fig. S13). POPC headgroup order parameters exhibit a clear decrease as a function of LiCl concentration but only modest changes as a function of KCl concentration, indicating significant Li⁺ binding but only weak K⁺ binding to the mixture when interpreted using the electrometer concept.^{31–33}

In simulations with Berger and CHARMM36 models, the responses of headgroup order parameter of both POPC and POPS to the added sodium or potassium are more similar to the experiments with LiCl (Fig. S13), indicating overestimated binding affinity of sodium and potassium in these simulations. The MacRog simulations with potassium exhibit weaker counterion binding affinity (Fig. S14), but significantly larger error bars and less systematic changes in the order parameters (Fig. S13). Similar unsystematic behaviour was also observed in the simulations of Lipid14/17 model with the additional counterions,^{22–25} for which the data is not shown due to the formation of ion clusters in water with relatively low (1 M) ion concentrations (Fig. S15). Appearance of such clusters also in the MagRog simulations with 4 M concentration of KCl could explain the unsystematic changes of the order parameters in this model with the added KCl. In conclusion, the results are in line with the section 25 in the main text, suggesting that the MacRog simulations with KCl give the most realistic

surface charge at the lipid bilayer interface among the tested simulation models.

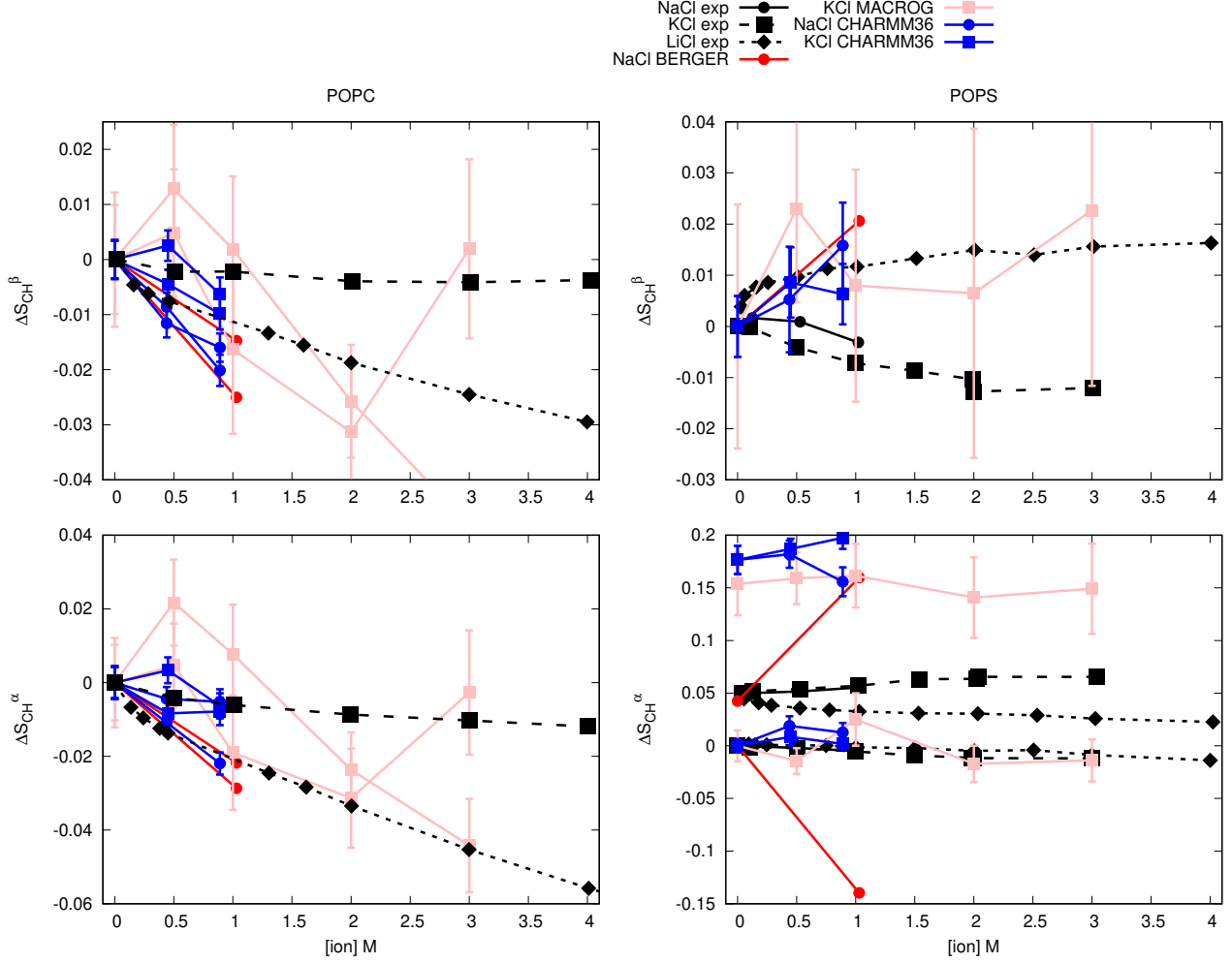


Figure S13: Changes of the PC (left) and PS (right) headgroup order parameters as a function of added NaCl, KCl and LiCl from POPC:POPS (5:1) mixture at 298 K (except Berger simulations are (4:1) mixture at 310 K). The experimental data is from Ref. 37. The values from counterion-only systems are set as a zero point of y-axis. To correctly illustrate the significant forking of the α -carbon order parameter in PS headgroup (bottom, right), the y-axis is transferred with the same value for both order parameters such that the lower order parameter value is at zero.

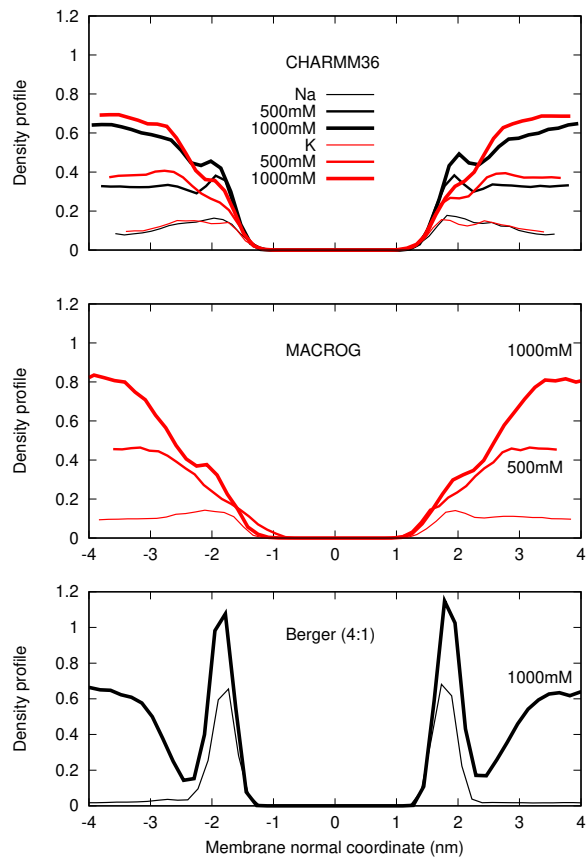


Figure S14: Counterion density distributions from PC:PS mixtures.

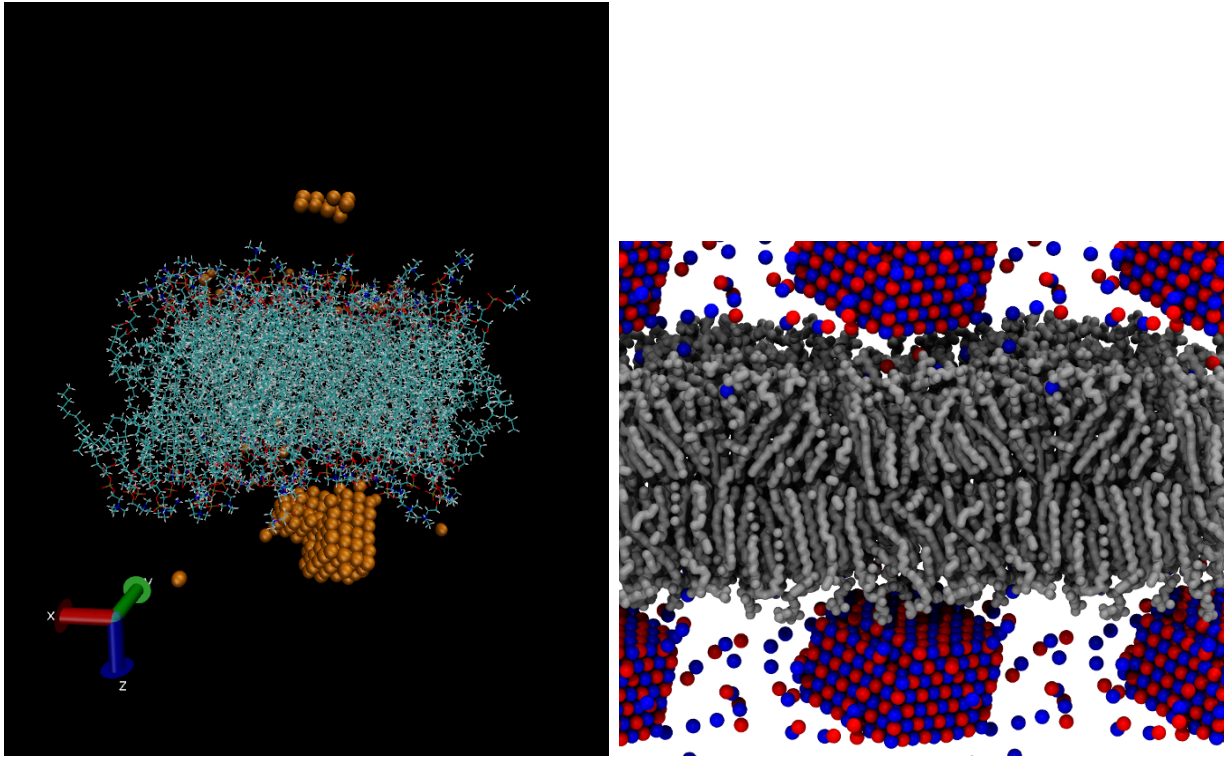


Figure S15: Ion clusters appearing in POPC:POPS (5:1) lipid17/14 simulations with 1 M of NaCl (left) and MacRog simulations with 4 M of KCl (right).

S8 Calcium binding to POPC in CHARMM36 simulation with NBfix

The response of POPC headgroup order parameters to the CaCl₂ concentration are underestimated in simulations of POPC:POPS (5:1) mixture with CHARMM36 containing the NBfix for interactions between calcium and lipid oxygens⁵³ (Fig. 9 in the main text), indicating that the calcium binding to the bilayer is too weak with these parameters. Without the NBfix term, the calcium binding affinity to pure POPC lipid bilayers was overestimated in the CHARMM36 model.⁴⁴ However, after employing the NBfix term, the response of headgroup order parameters (Fig. S16) and the binding affinity (Fig. S17) of calcium also to a pure POPC bilayer are underestimated. Notably, CHARMM36 simulations with the NBfix terms^{53,54} employed predict similar binding affinity for sodium and calcium. In conclusion, the special NBfix⁵³ for calcium, incorporated in the parameters give by the CHARMM-GUI at

the time of running the simulations (January 2018), leads to the underestimation of calcium binding affinity to pure PC and mixed PC:PS bilayers.

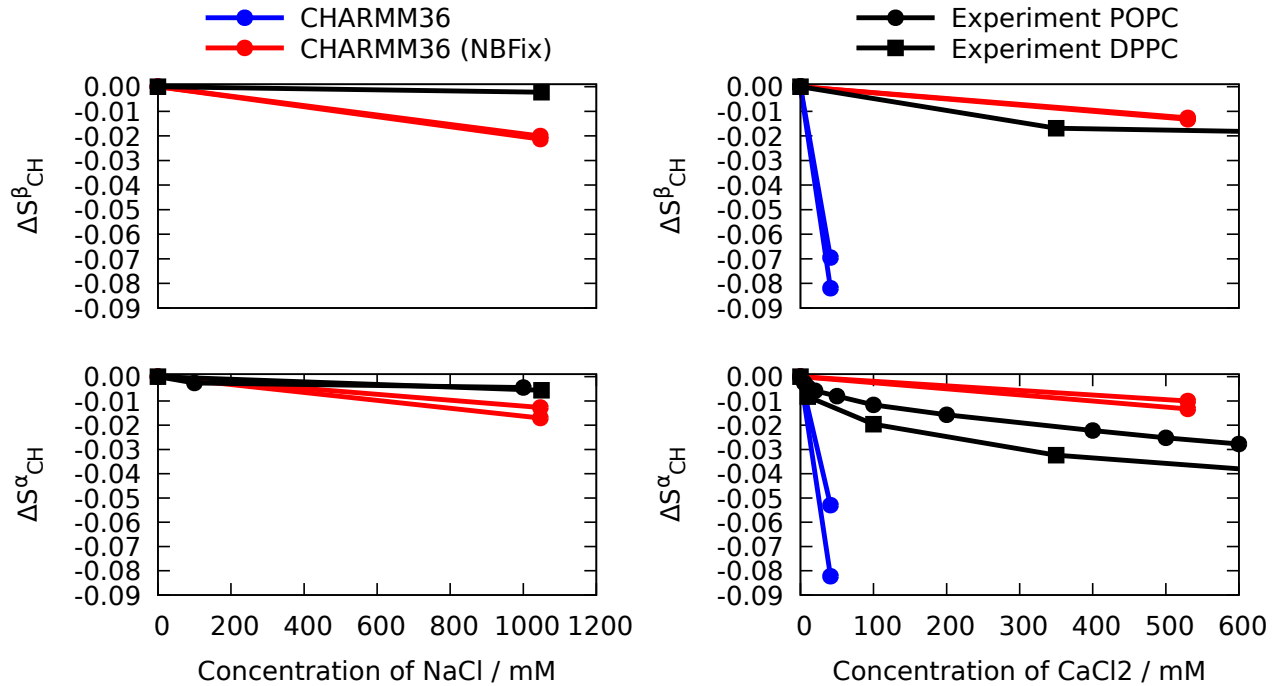


Figure S16: Headgroup order parameters from CHARMM36 simulations of POPC mixed with ions having the NBfix term employed for sodium⁵⁴ (*left*) and calcium⁵³ (*right*) compared with the experimental data^{31,32} and simulations without NBfix for the calcium. Simulation files without ions are available at Ref. 55, with the NBfix term in sodium at Ref. 56, with the NBfix term in calcium at Ref. 56 and without the NBfix in calcium at Ref. 57.

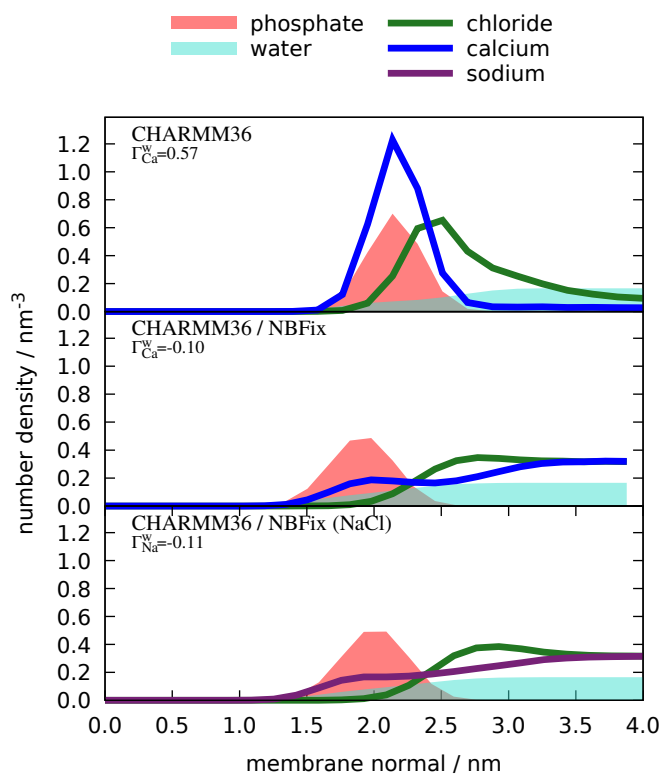


Figure S17: Density profiles along membrane normal from CHARMM36 simulations with (middle) and without (top) the NBfix term for calcium⁵³ compared to the simulation with the NBfix term for sodium⁵⁴ (bottom). The simulation data are the same as in figure S16.

S9 Calcium density profiles from simulations with POPC:POPS mixture

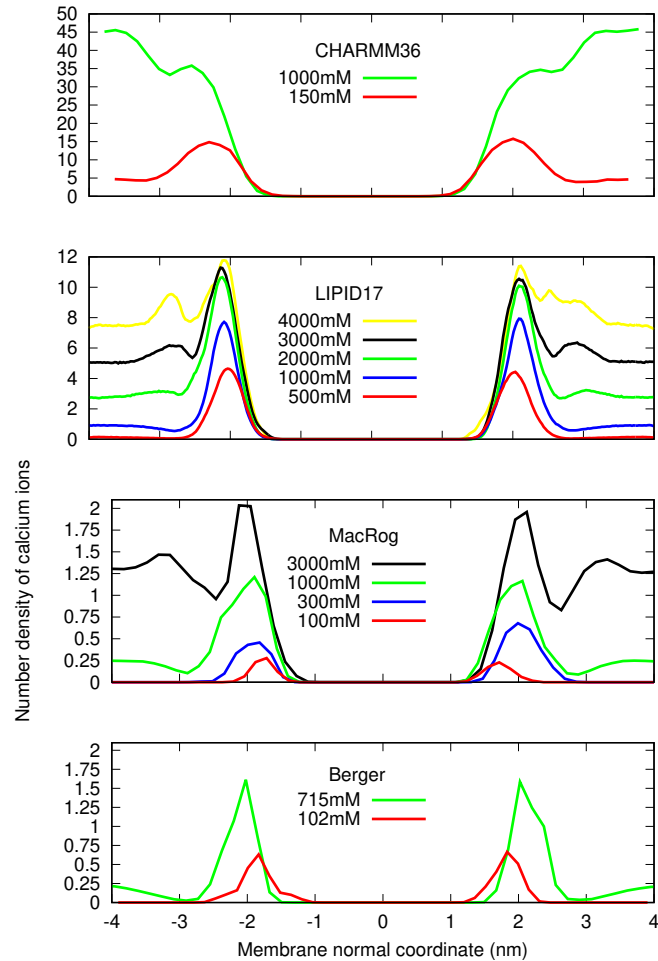


Figure S18: Ca^{2+} density profiles from simulations.

The CHARMM results are mass densities, number densities should be used when the data by Jesper Madsen is available.
Should we include also counterions into the plot?

S10 Details of the rough subjective force field ranking (Fig. 5)

The assessment was based fully on the Fig. 3. First, for each carbon (the columns in Fig. 3) in each force field (the rows), we looked separately at deviations in magnitude and forking.

Magnitude deviations, i.e., how close to the experimentally obtained C–H order parameters (OPs) the force-field-produced OPs were. For each carbon, the following 5-step scale was used:

0 (): More than half of all the calculated OPs (that is, of all different hydrogens in all different lipids) were within the *subjective sweet spots* (SSP, blue-shaded areas in Fig. 3).

1 (M): All the calculated OPs were < 0.03 units away from the SSP.

2 (M): All the calculated OPs were < 0.05 units away from the SSP.

3 (M): All the calculated OPs were < 0.10 units away from the SSP.

4 (M): Some of the calculated OPs were > 0.10 units away from the SSP.

Forking deviations, i.e., how well the difference in order parameters of two hydrogens attached to a given carbon matched that obtained experimentally. Note that this is not relevant for β and g_2 , which have only one hydrogen. For the α carbon, for which a considerable forking of 0.105 is experimentally seen, the following 5-step scale was used:

0 (): The distance D between the dots (that mark the measurement-time-weighted averages in Fig. 3) was $0.08 < D < 0.13$ units for all the calculated OPs (that is, for all different lipids).

1 (F): $(0.06 < D < 0.08)$ OR $(0.13 < D < 0.15)$.

2 (F): $(0.04 < D < 0.06)$ OR $(0.15 < D < 0.17)$.

3 (F): $(0.02 < D < 0.04)$ OR $(0.17 < D < 0.19)$.

4 (F): $(D < 0.02)$ OR $(0.19 < D)$.

For the g_3 carbon, for which no forking is indicated by experiments, the following 5-step scale was used:

0 (): $D < 0.02$.

1 (f): $0.02 < D < 0.04$.

2 (F): $0.04 < D < 0.06$.

3 (F): $0.06 < D < 0.08$.

4 (F): $0.08 < D$.

For the g_1 carbon, for which a considerable forking of 0.13 is experimentally seen, the following 5-step scale was used:

0 (): $0.11 < D < 0.15$.

1 (f): $(0.09 < D < 0.11)$ OR $(0.15 < D < 0.17)$.

2 (F): $(0.07 < D < 0.09)$ OR $(0.17 < D < 0.19)$.

3 (F): $(0.05 < D < 0.07)$ OR $(0.19 < D < 0.21)$.

4 (F): $(D < 0.05)$ OR $(0.21 < D)$.

Based on these assessments of magnitude and forking deviations, each carbon was then assigned to one of the following groups: "within experimental error" (magnitude and forking deviations both on step 0 of the scales described above), "almost within experimental error" (sum of the magnitude and forking deviation steps 1 or 2), "clear deviation from experiments" (sum of magnitude and forking deviation steps from 3 to 5), and "major deviation from experiments" (sum of magnitude and forking deviation steps from 6 to 8). These groups are

indicated by colors in Fig. 4. (Note that for β and g_2 , for which there can be no forking, the corresponding group assignment limits were: 0, 1, 2, and 3.)

Finally, the total ability of the force field to describe the headgroup and glycerol structure was estimated. To this end, the groups were given the following weights: 0 (within experimental error), 1 (almost within experimental error), 2 (clear deviation from experiments), 4 (major deviation from experiments), and the weights of the five carbons were summed up. The sum, given in the Σ -column of Fig. 3, was then used to (roughly and subjectively, as should be clear from the above description) rank the force fields.

References

- (1) Piggot, T. CHARMM36 DOPS simulations (versions 1 and 2) 303 K 1.0 nm LJ switching. 2017; <https://doi.org/10.5281/zenodo.1129411>.
- (2) Piggot, T. CHARMM36 POPS simulations (versions 1 and 2) 298 K 1.0 nm LJ switching. 2017; <https://doi.org/10.5281/zenodo.1129415>.
- (3) Piggot, T. CHARMM36 POPS simulations (versions 1 and 2) 298 K 1.0 nm LJ switching with K ions. 2018; <https://doi.org/10.5281/zenodo.1182654>.
- (4) Piggot, T. CHARMM36 POPS/POPC simulations (versions 1 and 2) 298 K 1.0 nm LJ switching with K ions. 2018; <https://doi.org/10.5281/zenodo.1182658>.
- (5) Piggot, T. CHARMM36 POPS/POPC simulations (versions 1 and 2) 298 K 1.0 nm LJ switching with Na ions. 2018; <https://doi.org/10.5281/zenodo.1182665>.
- (6) Lee, J.; Cheng, X.; Swails, J. M.; Yeom, M. S.; Eastman, P. K.; Lemkul, J. A.; Wei, S.; Buckner, J.; Jeong, J. C.; Qi, Y. et al. CHARMM-GUI Input Generator for NAMD, GROMACS, AMBER, OpenMM, and CHARMM/OpenMM Simulations Using the CHARMM36 Additive Force Field. *Journal of Chemical Theory and Computation* **2016**, *12*, 405–413.
- (7) Jo, S.; Kim, T.; Iyer, V. G.; Im, W. CHARMM-GUI: A web-based graphical user interface for CHARMM. *Journal of Computational Chemistry* **29**, 1859–1865.
- (8) Ollila, O. H. S. POPC:POPS (5:1) with 450 mM potassium simulation with CHARMM36 at 298K. 2018; <https://doi.org/10.5281/zenodo.1493241>.
- (9) Ollila, O. H. S. POPC:POPS (5:1) with 890 mM potassium simulation with CHARMM36 at 298K. 2018; <https://doi.org/10.5281/zenodo.1493246>.
- (10) Ollila, O. H. S. POPC:POPS (5:1) with 440 mM sodium simulation with CHARMM36 at 298K. 2018; <https://doi.org/10.5281/zenodo.1493190>.

- (11) Ollila, O. H. S. POPC:POPS (5:1) with 890 mM sodium simulation with CHARMM36 at 298K. 2018; <https://doi.org/10.5281/zenodo.1493229>.
- (12) Piggot, T. CHARMM36-UA DOPS simulations (versions 1 and 2) 303 K 1.0 nm LJ switching. 2017; <https://doi.org/10.5281/zenodo.1129456>.
- (13) Piggot, T. CHARMM36-UA POPS simulations (versions 1 and 2) 298 K 1.0 nm LJ switching. 2017; <https://doi.org/10.5281/zenodo.1129458>.
- (14) Piggot, T. MacRog POPS simulations (versions 1 and 2) 298 K with corrected PO not OP tails. 2018; <https://doi.org/10.5281/zenodo.1283335>.
- (15) Javanainen, M. Simulation of a POPS membrane with potassium counterions. 2018; <https://doi.org/10.5281/zenodo.1434990>.
- (16) Javanainen, M. Simulations of POPC/POPS membranes with CaCl₂. 2017; <https://doi.org/10.5281/zenodo.1409551>.
- (17) Javanainen, M. Simulations of POPC/POPS membranes with KCl. 2018; <https://doi.org/10.5281/zenodo.1404040>.
- (18) Miettinen, M. S.; Kav, B. Molecular dynamics simulation trajectory of an anionic lipid bilayer: 100 mol% POPS with Na⁺ counterions using Joung-Cheatham Ions. 2018; <https://doi.org/10.5281/zenodo.1148495>, B.K. acknowledges financial support from International Max Planck Research School on Multiscale Bio-Systems.
- (19) Miettinen, M. S.; Kav, B. Molecular dynamics simulation trajectory of an anionic lipid bilayer: 100 mol% POPS with Na⁺ counterions using ff99 ions. 2018; <https://doi.org/10.5281/zenodo.1134869>, B.K. acknowledges financial support from International Max Planck Research School on Multiscale Bio-Systems.
- (20) Kav, B.; Miettinen, M. S. Molecular dynamics simulation trajectory of an anionic lipid bilayer: 100 mol% DOPS with Na⁺ counterions using Joung-Cheetham Ions. 2018;

<https://doi.org/10.5281/zenodo.1134871>, B.K acknowledges financial support from International Max Planck Research School on Multiscale Bio-Systems.

- (21) Kav, B.; Miettinen, M. S. Molecular dynamics simulation trajectory of an anionic lipid bilayer: 100 mol% DOPS with Na⁺ counterions using ff99 Ions. 2018; <https://doi.org/10.5281/zenodo.1135142>, B.K acknowledges financial support from International Max Planck Research School on Multiscale Bio-Systems.
- (22) Kav, B.; Miettinen, M. S. Amber Lipid17 Simulations of POPC/POPS Membranes with KCl Counterions. 2018; <https://doi.org/10.5281/zenodo.1250969>, B.K acknowledges financial support from International Max Planck Research School on Multiscale Bio-Systems.
- (23) Kav, B.; Miettinen, M. S. Amber Lipid17 Simulations of POPC/POPS Membranes with KCl. 2018; <https://doi.org/10.5281/zenodo.1227257>, B.K acknowledges financial support from International Max Planck Research School on Multiscale Bio-Systems.
- (24) Kav, B.; Miettinen, M. S. Amber Lipid17 Simulations of POPC/POPS Membranes with NaCl Counterions. 2018; <https://doi.org/10.5281/zenodo.1250975>, B.K acknowledges financial support from International Max Planck Research School on Multiscale Bio-Systems.
- (25) Kav, B.; Miettinen, M. S. Amber Lipid17 Simulations of POPC/POPS Membranes with NaCl. 2018; <https://doi.org/10.5281/zenodo.1227272>, B.K acknowledges financial support from International Max Planck Research School on Multiscale Bio-Systems.
- (26) Melcr, J. Molecular dynamics simulations of lipid bilayers containing POPC and POPS with the lipid17 force field, only counterions, and CaCl₂ concentrations. 2018; <https://doi.org/10.5281/zenodo.1487761>.
- (27) Jurkiewicz, P.; Cwiklik, L.; Vojtíšková, A.; Jungwirth, P.; Hof, M. Structure, dynamics,

- and hydration of POPC/POPS bilayers suspended in NaCl, KCl, and CsCl solutions. *Biochimica et Biophysica Acta (BBA) - Biomembranes* **2012**, *1818*, 609 – 616.
- (28) Melcrová, A.; Pokorna, S.; Pullanchery, S.; Kohagen, M.; Jurkiewicz, P.; Hof, M.; Jungwirth, P.; Cremer, P. S.; Cwiklik, L. The complex nature of calcium cation interactions with phospholipid bilayers. *Sci. Reports* **2016**, *6*, 38035.
- (29) Ollila, S.; Hyvönen, M. T.; Vattulainen, I. Polyunsaturation in Lipid Membranes: Dynamic Properties and Lateral Pressure Profiles. *J. Phys. Chem. B* **2007**, *111*, 3139–3150.
- (30) Mukhopadhyay, P.; Monticelli, L.; Tielemans, D. P. Molecular Dynamics Simulation of a Palmitoyl-Oleoyl Phosphatidylserine Bilayer with Na⁺ Counterions and NaCl. *Biophysical Journal* **2004**, *86*, 1601 – 1609.
- (31) Akutsu, H.; Seelig, J. Interaction of metal ions with phosphatidylcholine bilayer membranes. *Biochemistry* **1981**, *20*, 7366–7373.
- (32) Altenbach, C.; Seelig, J. Calcium binding to phosphatidylcholine bilayers as studied by deuterium magnetic resonance. Evidence for the formation of a calcium complex with two phospholipid molecules. *Biochemistry* **1984**, *23*, 3913–3920.
- (33) Seelig, J.; MacDonald, P. M.; Scherer, P. G. Phospholipid head groups as sensors of electric charge in membranes. *Biochemistry* **1987**, *26*, 7535–7541.
- (34) Scherer, P. G.; Seelig, J. Electric charge effects on phospholipid headgroups. Phosphatidylcholine in mixtures with cationic and anionic amphiphiles. *Biochemistry* **1989**, *28*, 7720–7728.
- (35) Borle, F.; Seelig, J. Ca²⁺ binding to phosphatidylglycerol bilayers as studied by differential scanning calorimetry and ²H- and ³¹P-nuclear magnetic resonance. *Chemistry and Physics of Lipids* **1985**, *36*, 263 – 283.

- (36) Macdonald, P. M.; Seelig, J. Calcium binding to mixed phosphatidylglycerol-phosphatidylcholine bilayers as studied by deuterium nuclear magnetic resonance. *Biochemistry* **1987**, *26*, 1231–1240.
- (37) Roux, M.; Bloom, M. Calcium, magnesium, lithium, sodium, and potassium distributions in the headgroup region of binary membranes of phosphatidylcholine and phosphatidylserine as seen by deuterium NMR. *Biochemistry* **1990**, *29*, 7077–7089.
- (38) Roux, M.; Neumann, J.-M. Deuterium NMR study of head-group deuterated phosphatidylserine in pure and binary phospholipid bilayers. *FEBS Letters* **1986**, *199*, 33–38.
- (39) Roux, M.; Bloom, M. Calcium binding by phosphatidylserine headgroups. Deuterium NMR study. *Biophys. J.* **1991**, *60*, 38 – 44.
- (40) Scherer, P.; Seelig, J. Structure and dynamics of the phosphatidylcholine and the phosphatidylethanolamine head group in L-M fibroblasts as studied by deuterium nuclear magnetic resonance. *EMBO J.* **1987**, *6*.
- (41) Ferreira, T. M.; Coreta-Gomes, F.; Ollila, O. H. S.; Moreno, M. J.; Vaz, W. L. C.; Topgaard, D. Cholesterol and POPC segmental order parameters in lipid membranes: solid state ^1H - ^{13}C NMR and MD simulation studies. *Phys. Chem. Chem. Phys.* **2013**, *15*, 1976–1989.
- (42) Ollila, O. S.; Pabst, G. Atomistic resolution structure and dynamics of lipid bilayers in simulations and experiments. *Biochimica et Biophysica Acta (BBA) - Biomembranes* **2016**, *1858*, 2512 – 2528.
- (43) Ferreira, T. M.; Sood, R.; Bärenwald, R.; Carlström, G.; Topgaard, D.; Saalwächter, K.; Kinnunen, P. K. J.; Ollila, O. H. S. Acyl Chain Disorder and Azelaoyl Orientation in Lipid Membranes Containing Oxidized Lipids. *Langmuir* **2016**, *32*, 6524–6533.

- (44) Catte, A.; Girych, M.; Javanainen, M.; Loison, C.; Melcr, J.; Miettinen, M. S.; Monticelli, L.; Maatta, J.; Oganesyan, V. S.; Ollila, O. H. S. et al. Molecular electrometer and binding of cations to phospholipid bilayers. *Phys. Chem. Chem. Phys.* **2016**, *18*, 32560–32569.
- (45) Melcr, J.; Martinez-Seara, H.; Nencini, R.; Kolafa, J.; Jungwirth, P.; Ollila, O. H. S. Accurate Binding of Sodium and Calcium to a POPC Bilayer by Effective Inclusion of Electronic Polarization. *The Journal of Physical Chemistry B* **2018**, *122*, 4546–4557.
- (46) Ollila, O. H. S. CHARMM36 simulations of POPC mixed with cationic surfactant. 2018; <https://doi.org/10.5281/zenodo.1288297>.
- (47) Melcr, J. POPC lipid membrane, 303K, Charmm36 force field, simulation files and 200 ns trajectory for Gromacs MD simulation engine v5.1.2. 2016; <https://doi.org/10.5281/zenodo.153944>.
- (48) Favela-Rosales, F. MD simulation trajectory of a lipid bilayer: Pure POPC in water. SLIPIDS, Gromacs 4.6.3. 2016. 2016; <https://doi.org/10.5281/zenodo.166034>.
- (49) Hauser, H.; Shipley, G. G. Interactions of monovalent cations with phosphatidylserine bilayer membranes. *Biochemistry* **1983**, *22*, 2171–2178.
- (50) Hauser, H.; Shipley, G. Comparative structural aspects of cation binding to phosphatidylserine bilayers. *Biochimica et Biophysica Acta (BBA) - Biomembranes* **1985**, *813*, 343 – 346.
- (51) Mattai, J.; Hauser, H.; Demel, R. A.; Shipley, G. G. Interactions of metal ions with phosphatidylserine bilayer membranes: effect of hydrocarbon chain unsaturation. *Biochemistry* **1989**, *28*, 2322–2330.
- (52) Cevc, G. Membrane electrostatics. *Biochim. Biophys. Acta - Rev. Biomemb.* **1990**, *1031*, 311 – 382.

- (53) Kim, S.; Patel, D.; Park, S.; Slusky, J.; Klauda, J.; Widmalm, G.; Im, W. Bilayer Properties of Lipid A from Various Gram-Negative Bacteria. *Biophysical Journal* **2016**, *111*, 1750 – 1760.
- (54) Venable, R. M.; Luo, Y.; Gawrisch, K.; Roux, B.; Pastor, R. W. Simulations of Anionic Lipid Membranes: Development of Interaction-Specific Ion Parameters and Validation Using NMR Data. *The Journal of Physical Chemistry B* **2013**, *117*, 10183–10192.
- (55) Nencini, R. Simulation data for CHARMM36 POPC bilayer, 100 lipids/leaflet, 310K, GROMACS 5.1.4. 2018; <https://doi.org/10.5281/zenodo.1198158>.
- (56) Nencini, R. Simulation data for CHARMM36 POPC bilayer, 100 lipids/leaflet, 450 mM CaCl₂ ("NB-Fix" used), 310K, GROMACS 5.1.4. 2018; <https://doi.org/10.5281/zenodo.1198171>.
- (57) Javanainen, M. POPC @ 310K, 450 mM of CaCl₂. Charmm36 with default Charmm ions. 2016; <http://dx.doi.org/10.5281/zenodo.51185>.